Supplementary Information (SI) for New Journal of Chemistry.
This journal is © The Royal Society of Chemistry and the Centre National de la Recherche Scientifique 2025

Supporting information

Structural and Antimicrobial Studies on Tricarbonyl Rhenium(I) Complex with 6,7-Dimethyl-2-(pyridin-2-yl)quinoxaline Ligand

Sibusiso A. Sithole, [a] Ahmed M. Mansour, [b,c*] Frederick P. Malan, [d] Gurusamy Manikandan, [e] David R. Katerere, [e] Ola R Shehab,[b] and Amanda-Lee E. Manicum [a*]

[a] Department of Chemistry, Tshwane University of Technology, Pretoria 0001, South Africa.

[b] Department of Chemistry, Faculty of Science, Cairo University, Gamma Street, Giza, 12613, Egypt. mansour@sci.cu.edu.eg.

[c] Department of Chemistry, United Arab Emirates University, Al-Ain, United Arab Emirates.

[d] Department of Chemistry, University of Pretoria, Pretoria 0001, South Africa

[e] Department of Pharmaceutical Sciences, Tshwane University of Technology, Pretoria 0001, South Africa (PB2A)

*Corresponding author's email: ManicumAE@tut.ac.za (Manicum) ; mansour@sci.cu.edu.eg (Mansour)

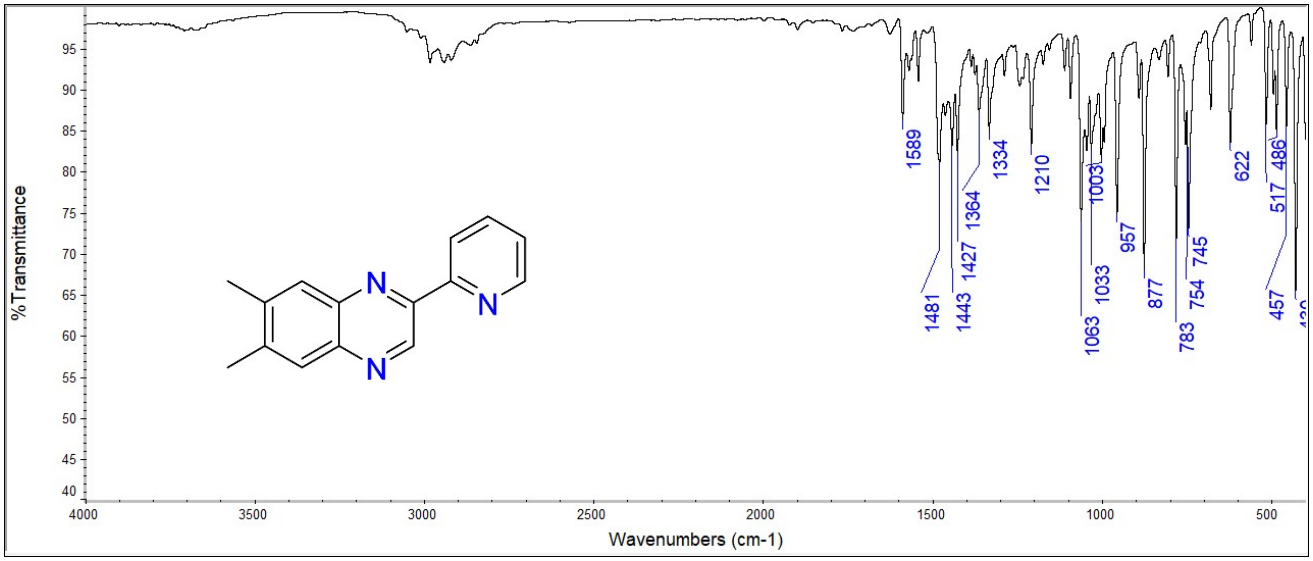

Fig. S1 Fourier Transform infrared spectrum of **1**.

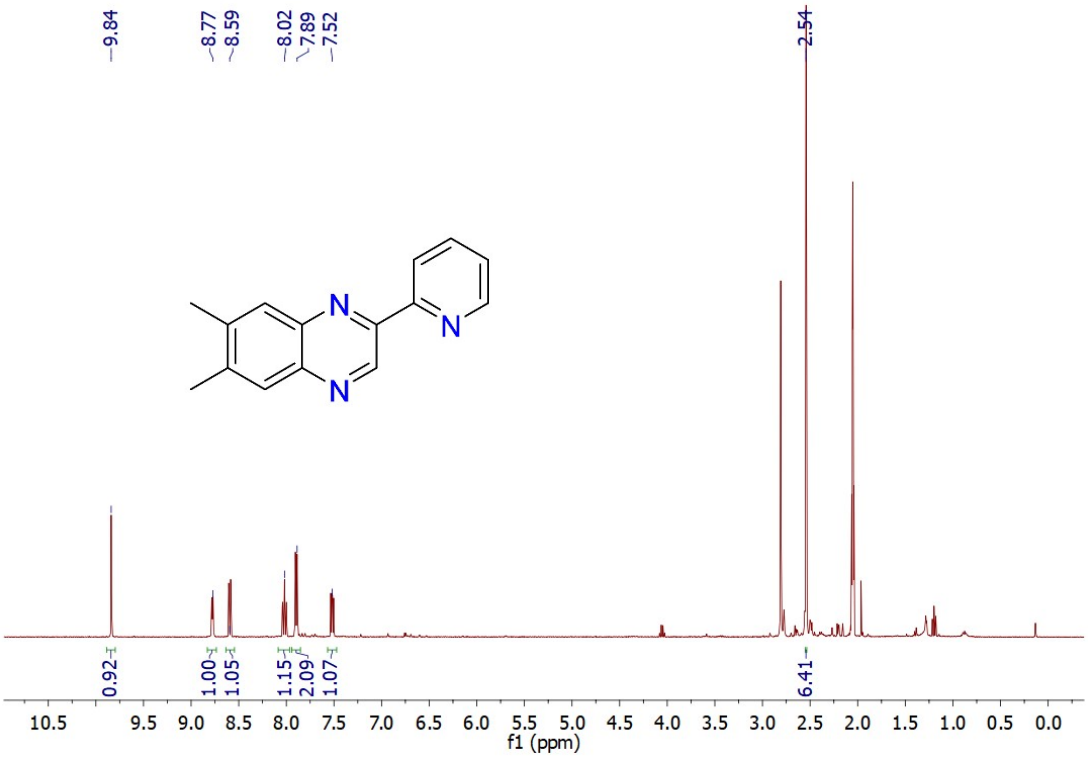

a)

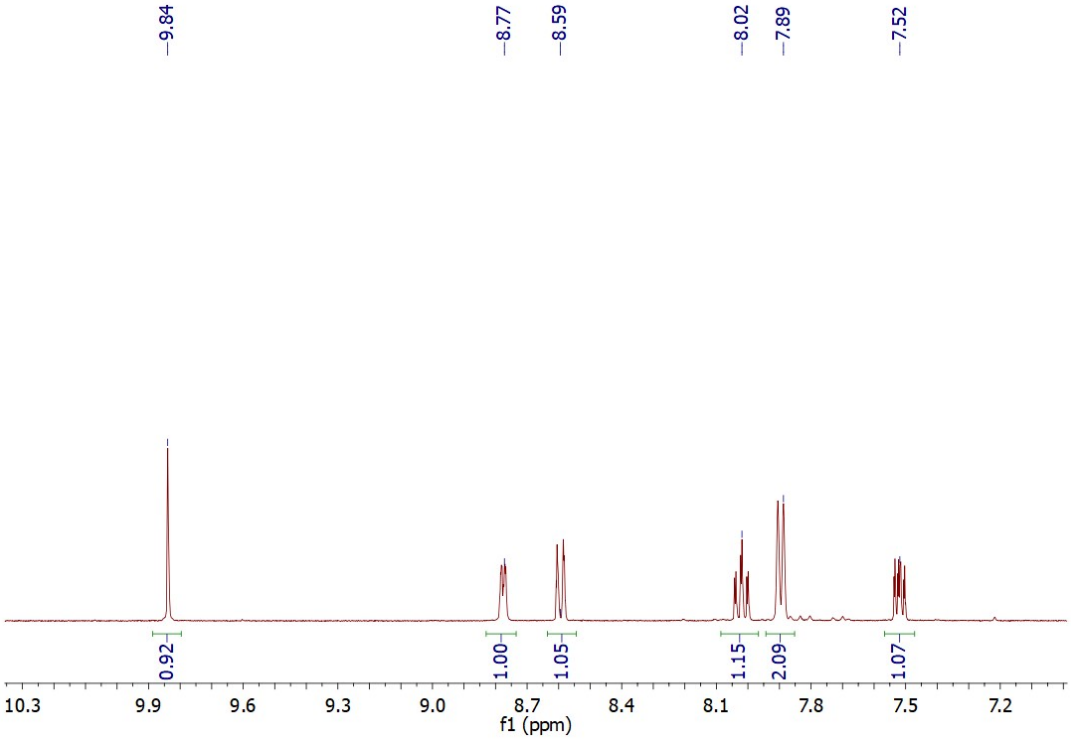

b)

Fig. S2 ^{1}H NMR spectra of **1** in acetone-d_6 **a)** Full spectrum and **b)** Aromatic region.

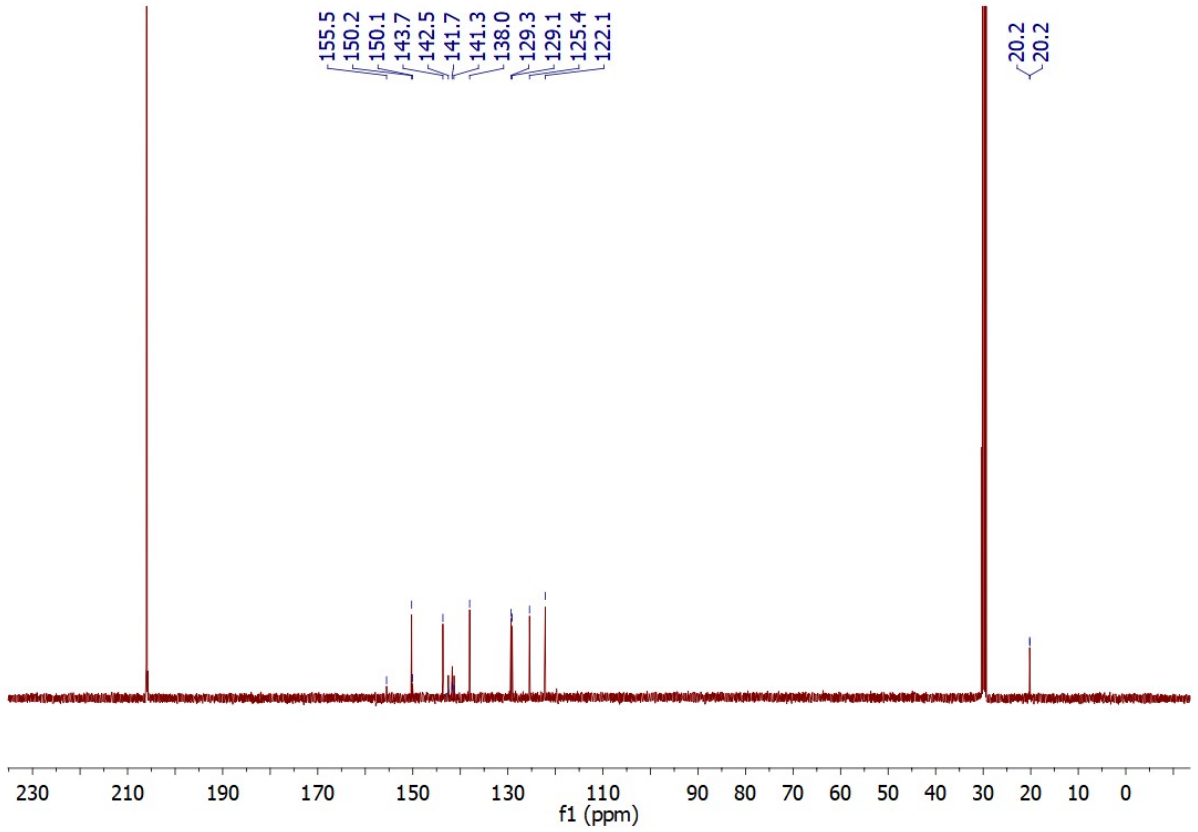

Fig. S3 ^{13}C NMR spectra of **1** in Acetone-d_6.

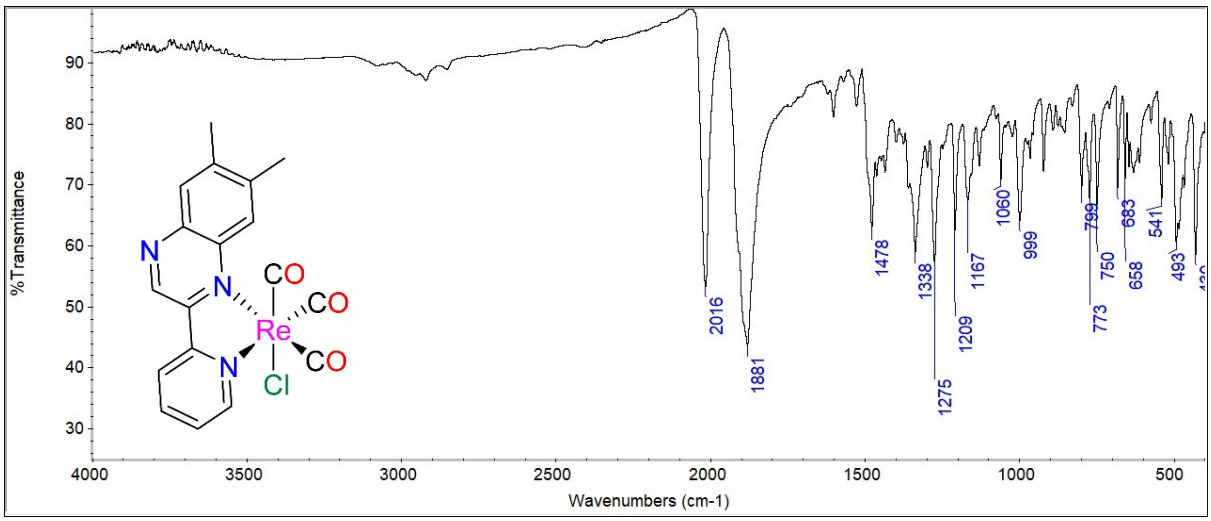

Fig. S4 FT-IR spectrum of **2.**

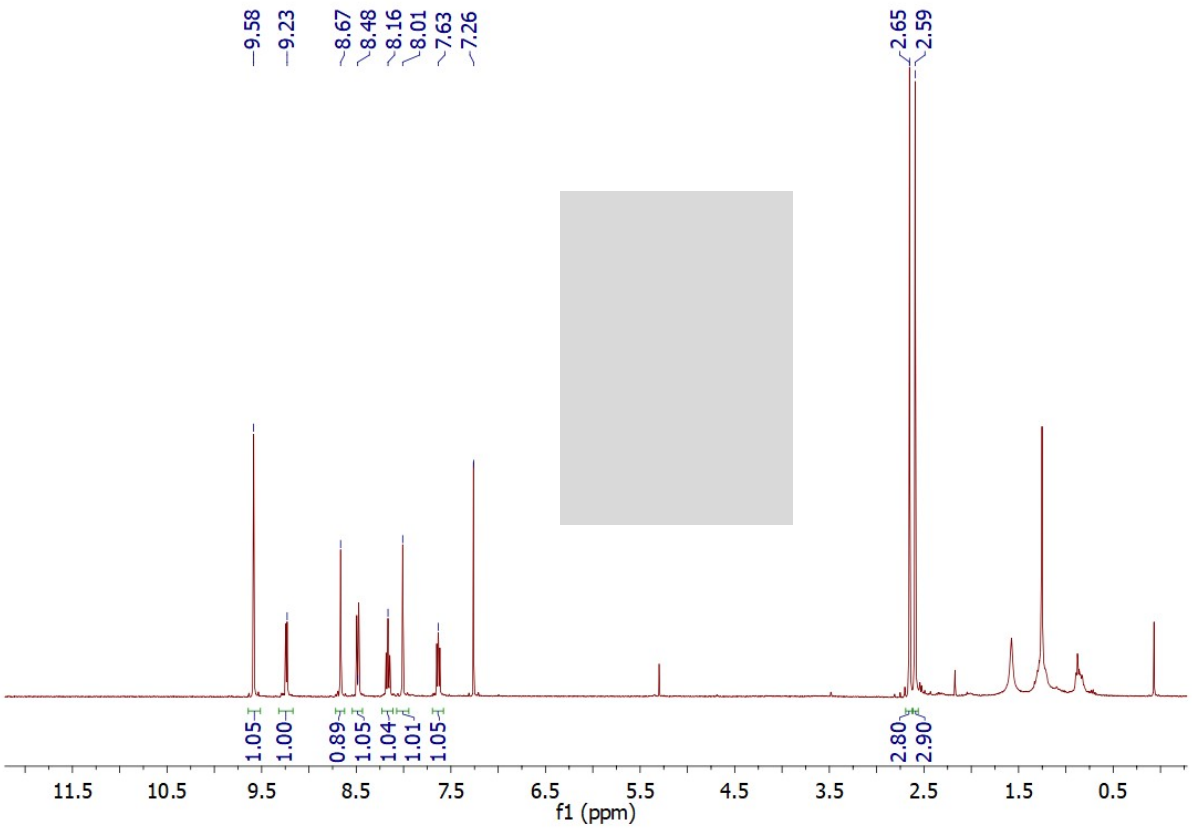

a)

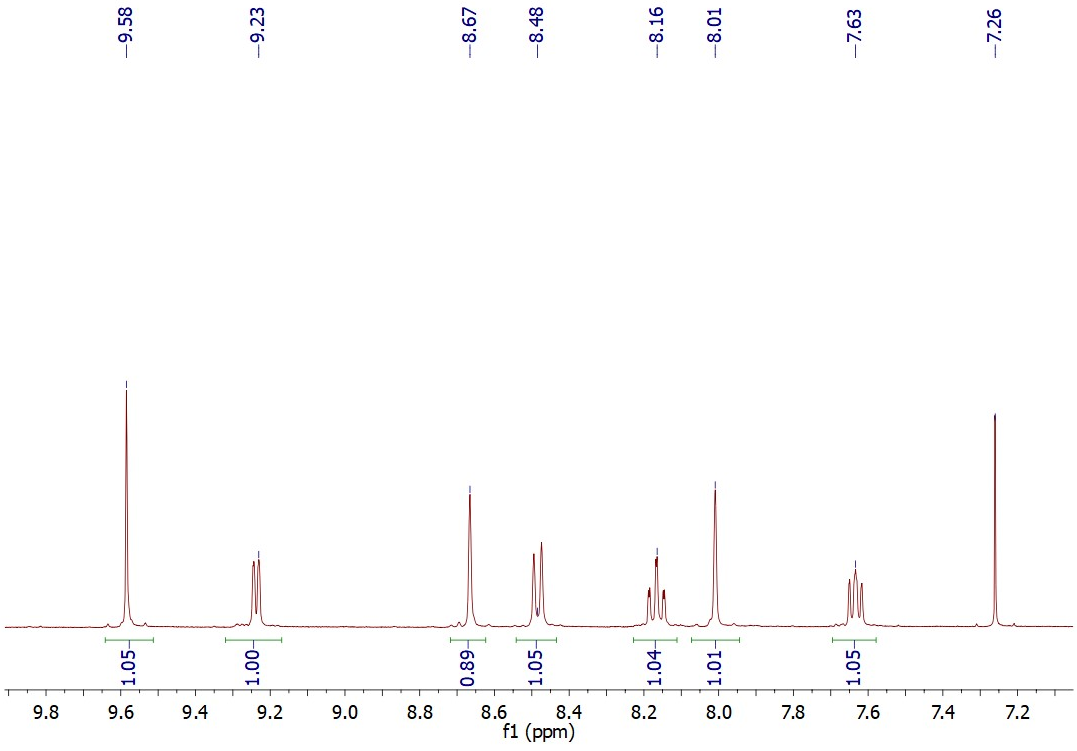

b)

Fig. S5 ^{1}H NMR spectra of **2** in $CDCl_3$ **a)** Full spectrum and **b)** Aromatic region.

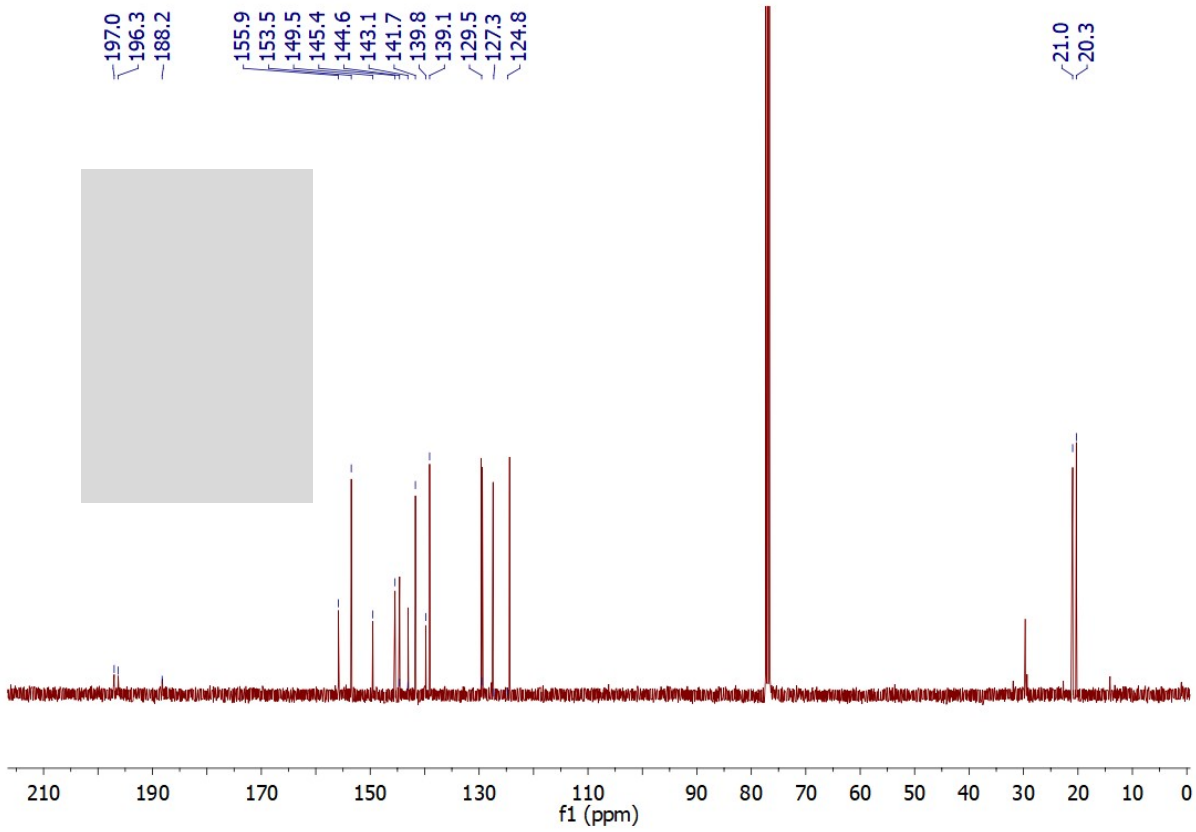

Fig. S6 ^{13}C NMR spectra of **2** in $CDCl_3$.

Table S1 Crystallographic data for **1** and **2**.

Crystallographic data	**1**	**2**
Empirical formula	$C_{15}H_{13}N_3$	$2(C_{18}H_{14}ClN_3O_{3.5}Re)$
CCDC No.	2433822	2433551
Molecular weight	235.28	1099.94
Temperature (K)	150.00(10)	100.00(2)
Crystal system	orthorhombic	orthorhombic
Space group	*Pbca*	$Pca2_1$
Z	8	4
a (Å)	11.9662(4)	7.4384(3)
b (Å)	7.4448(3)	15.5722(6)
c (Å)	26.0051(9)	29.4061(11)
α (°)	90	90
β (°)	90	90
γ (°)	90	90
Volume (Å^3)	2316.69(15)	3406.2(2)
ρ_{calc}g (cm^3)	1.349	2.145
μ (mm^{-1})	0.083	7.320
F(000)	992.0	2104.0
Reflections collected	22431	45010
Independent reflections	3121	8332

Data/restraints/parameters	3121/0/165	8332/1/486
R_1/ wR_2	0.0406/ 0.1222	0.0272/ 0.0613
Goodness of fit on F^2	1.049	1.188
Largest diff. peak/hole ($eÅ^{-3}$)	0.34/-0.20	1.59/-1.97

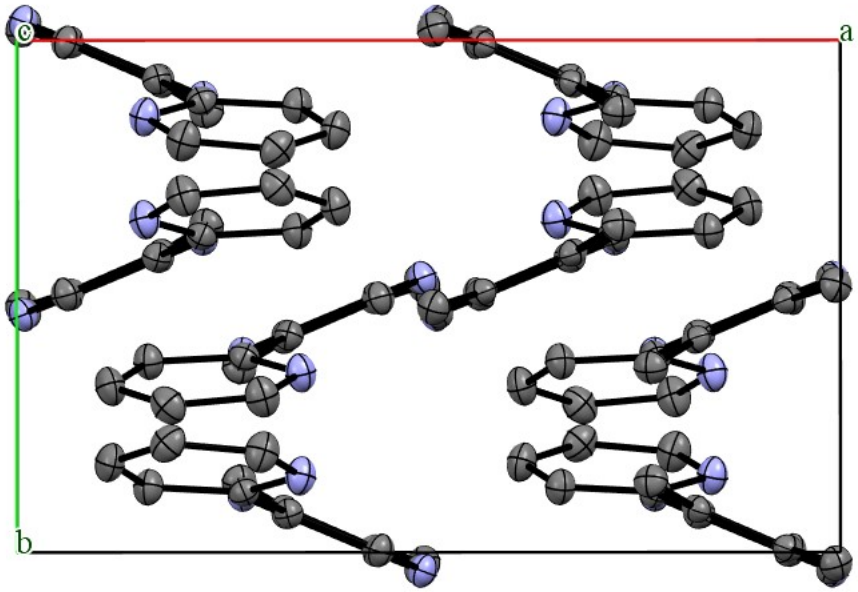

Fig. S7 The unit cell of **1**.

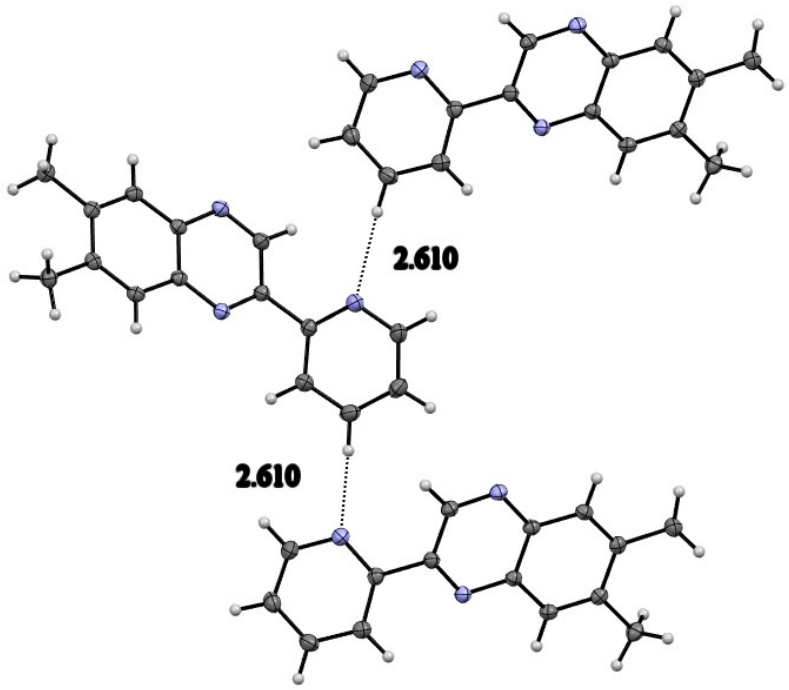

Fig. S8 non-covalent intermolecular interactions stabilizing the crystal packing of **1**.

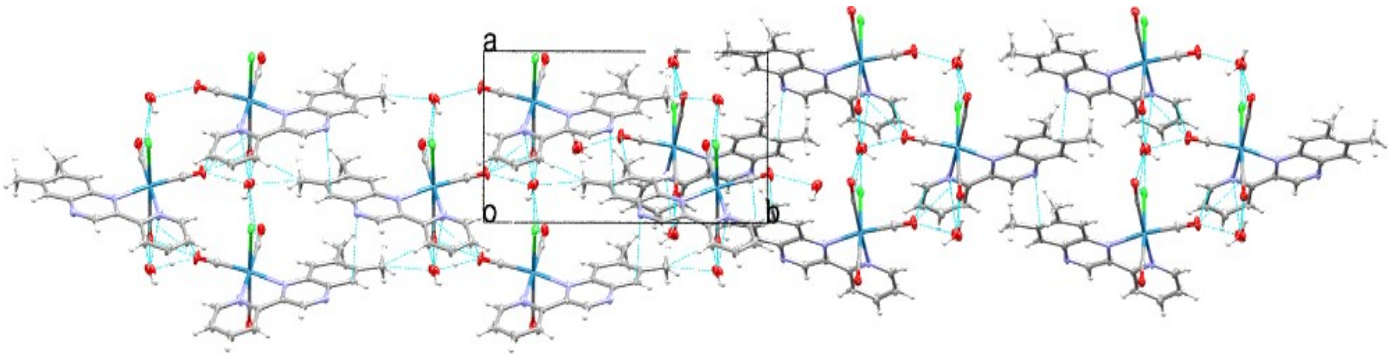

Figure S9. Packing diagram of **2** as viewed along the *c* axis. Hydrogen bonds are indicated using teal dotted lines.

Table S2 Selected bond lengths and angles of **1** and **2**.

1		**2**	
Experimental (Å/°)	Theoretical (Å/°)	Experimental (Å/°)	Theoretical (Å/°)
C1−C2 = 1.483(1)	1.489	Re1A−N1A = 2.171(7)	2.16308
C2−C3 = 1.429(1)	1.426	Re1A−N2A = 2.213(6)	2.20714
N1−C1 = 1.341(1)	1.339	Re1A−Cl1A = 2.501(2)	2.54677
N2−C2 = 1.319(1)	1.316	Re1A−C1A = 1.934(9)	1.92970
N3−C3 = 1.314(1)	1.310	Re1A−C2A = 1.916(8)	1.92038

C1−C10 = 1.394(1)	1.399	Re1A−C3A = 1.935(10)	1.91115
C6-C6A1 = 1.507(1)		C1A−O2 = 1.135(11)	1.18526
		C2A−O1 = 1.139(10)	1.18648
C2−N2−C9 = 116.53(9)	117.30	C3A−O3 = 1.130(12)	1.19228
C3-N3-C4 = 116.05(9)	116.68	Re1B−N1B = 2.155(7)	2.16308
C13-N1-C1 = 117.26(9)	118.14	Re1B−N2B = 2.225(6)	2.20714
N2-C2-C1 = 117.89(9)	118.58	Re1B−Cl1B = 2.502(2)	2.54677
		Re1B−C1B = 1.931(9)	1.92970
		Re1B−C2B = 1.906(8)	1.92038
		Re1B−C3B = 1.907(9)	1.91115
		C1B−O6 = 1.125(11)	1.18526
		C2B−O8 = 1.146(10)	1.18648
		C3B−O7 = 1.159(11)	1.19228
		N1A−Re1A−Cl1A = 84.81(19)	170.75
		N1A−Re1A−N2A = 74.7(3)	75.38
		N2A−Re1A−Cl1A = 83.43(16)	101.33
		C2A−Re1A−Cl1A = 93.0(3)	87.94
		C2A−Re1A−N1A = 94.6(3)	94.51
		C2A−Re1A−N2A = 169.0(3)	168.88
		C1A−Re1A−N2A = 105.6(3)	

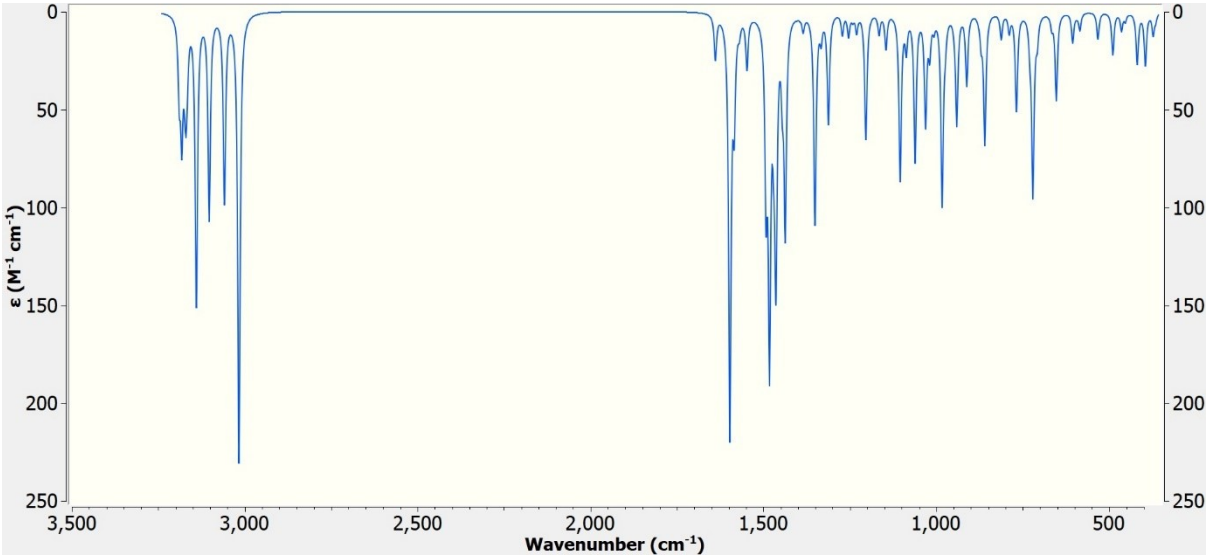

a)

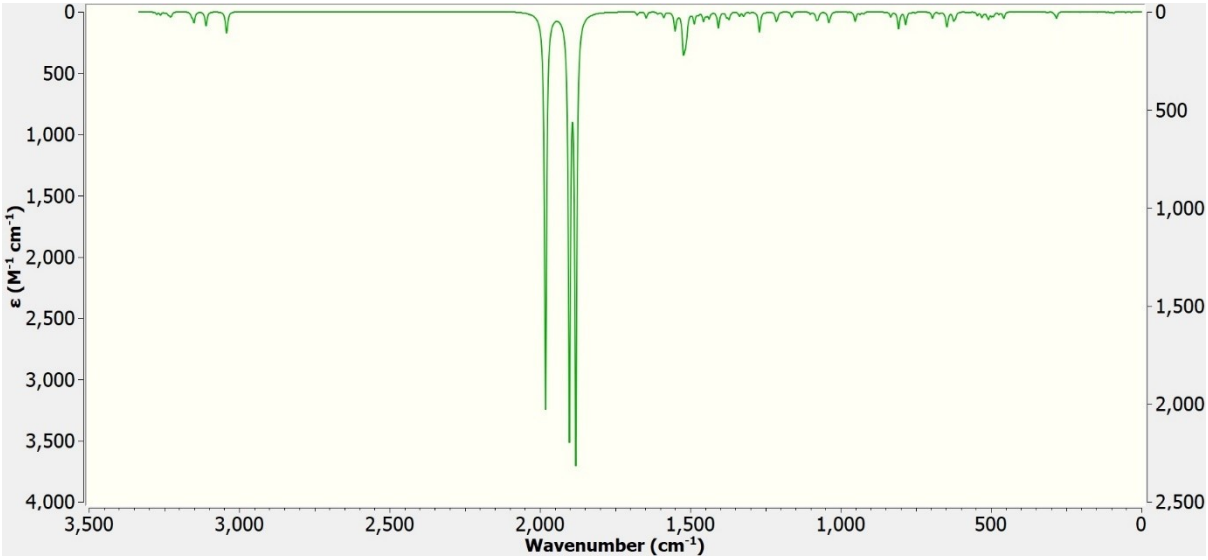

b)

Fig. S10 Theoretical infrared spectra of **1** and **2** obtained at B3LYP/6-311+G(2d,p) and B3LYP/LANL2DZ level of theories.

Table S3 Atomic coordinates of the optimized structure of ligand **1**

Center number*	Atomic number	Atomic type	Coordinates (Å)		
			X	Y	Z
1	6	0	-3.730712	-0.355222	-0.026148
2	6	0	1.198762	-0.348394	-0.057508
3	6	0	2.650351	-0.017714	-0.015388
4	6	0	-1.970818	1.304871	0.171449
5	1	0	-1.627485	2.324874	0.298536
6	7	0	3.031191	1.133381	-0.584361
7	7	0	0.326401	0.628973	0.069353
8	6	0	-1.405094	-1.049911	-0.138108
9	6	0	-0.987212	0.298246	0.032446
10	6	0	-3.311319	1.006166	0.146159
11	6	0	-2.785791	-1.343611	-0.163283
12	1	0	-3.077111	-2.379073	-0.296448
13	6	0	-5.19708	-0.698074	-0.058787

14	1	0	-5.699352	-0.403423	0.867272
15	1	0	-5.343664	-1.769464	-0.194892
16	1	0	-5.711475	-0.181245	-0.874333
17	6	0	3.562195	-0.881309	0.600912
18	1	0	3.221975	-1.794029	1.073248
19	7	0	-0.490942	-2.045676	-0.280573
20	6	0	4.32274	1.450813	-0.554813
21	1	0	4.592789	2.389128	-1.030652
22	6	0	0.770766	-1.696165	-0.239058
23	1	0	1.503469	-2.485886	-0.375336
24	6	0	5.301322	0.655765	0.035649
25	1	0	6.338398	0.967204	0.029579
26	6	0	4.906163	-0.535701	0.627343
27	1	0	5.629488	-1.183867	1.107805
28	6	0	-4.335657	2.10029	0.297683
29	1	0	-4.999645	2.151504	-0.570055
30	1	0	-3.85411	3.071476	0.410476
31	1	0	-4.971518	1.935757	1.172567
Rotational constants (GHz)			1.369638	0.196299	0.175137

Table S4 Atomic coordinates of the optimized structure of ligand **2**

Center number*	Atomic number	Atomic type	Coordinates (Å)		
			X	Y	Z
1	75	0	-0.927482	-0.862354	-0.005245
2	17	0	-1.116605	-0.088304	-2.424155
3	8	0	-3.400532	-2.71325	-0.331536
4	8	0	0.857471	-3.209325	-1.008211
5	8	0	-0.621924	-1.64799	2.981512
6	6	0	4.783208	0.603943	0.037964
7	6	0	-0.739287	-1.347277	1.83376
8	6	0	0.191655	-2.315432	-0.605126
9	6	0	-0.027051	2.022376	0.025512
10	6	0	-1.487568	2.104785	0.179164
11	6	0	-2.436874	-2.031575	-0.21144
12	6	0	2.614606	-0.514083	0.329702
13	1	0	2.043745	-1.40497	0.548174

14	7	0	-2.126595	0.902379	0.350818
15	7	0	0.532906	0.788125	0.115883
16	6	0	2.705053	1.899185	-0.103365
17	6	0	1.923275	0.706058	0.110423
18	6	0	4.004262	-0.585801	0.299231
19	6	0	4.122194	1.811971	-0.148363
20	1	0	4.666788	2.733646	-0.328728
21	6	0	6.294576	0.535013	-0.020508
22	1	0	6.71747	0.178264	0.928683
23	1	0	6.72726	1.517061	-0.234858
24	1	0	6.631987	-0.161046	-0.800393
25	6	0	-2.205245	3.316743	0.209421
26	1	0	-1.695295	4.261924	0.069357
27	7	0	2.109861	3.133255	-0.259014
28	6	0	-3.469167	0.887974	0.567319
29	1	0	-3.930643	-0.08245	0.696041
30	6	0	0.784072	3.183298	-0.170036
31	1	0	0.329322	4.161401	-0.274919
32	6	0	-4.233005	2.060195	0.611045
33	1	0	-5.302154	1.99614	0.781839
34	6	0	-3.59024	3.297282	0.42151
35	1	0	-4.154843	4.224562	0.440537
36	6	0	4.694405	-1.912787	0.535372
37	1	0	5.287404	-2.211936	-0.339807
38	1	0	3.969691	-2.707611	0.733543
39	1	0	5.386193	-1.860263	1.3871
Rotational constants (GHz)			0.2565712	0.1411797	0.1081313

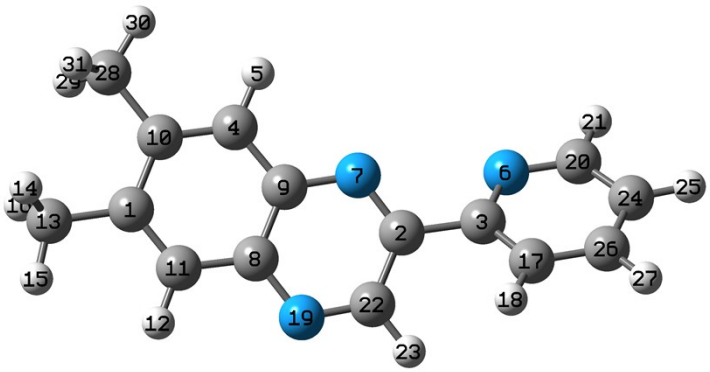

a)

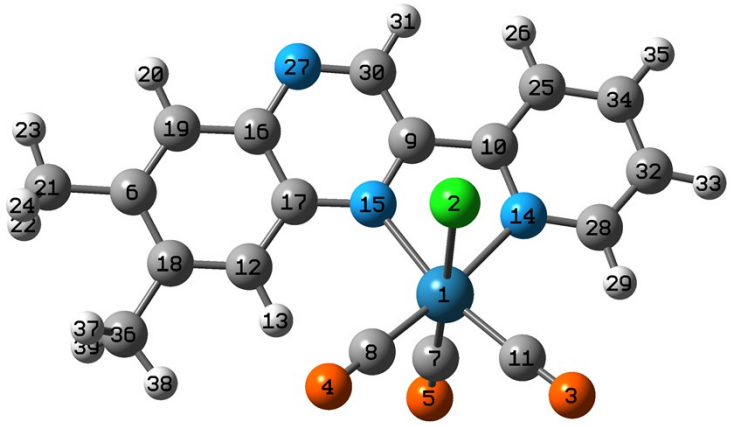

b)

Fig. S11 The local minimum structures of a) **1** and b) **2** calculated at B3LYP/6-311+G(2d, p) and B3LYP/LANL2DZ level of theory, respectively.

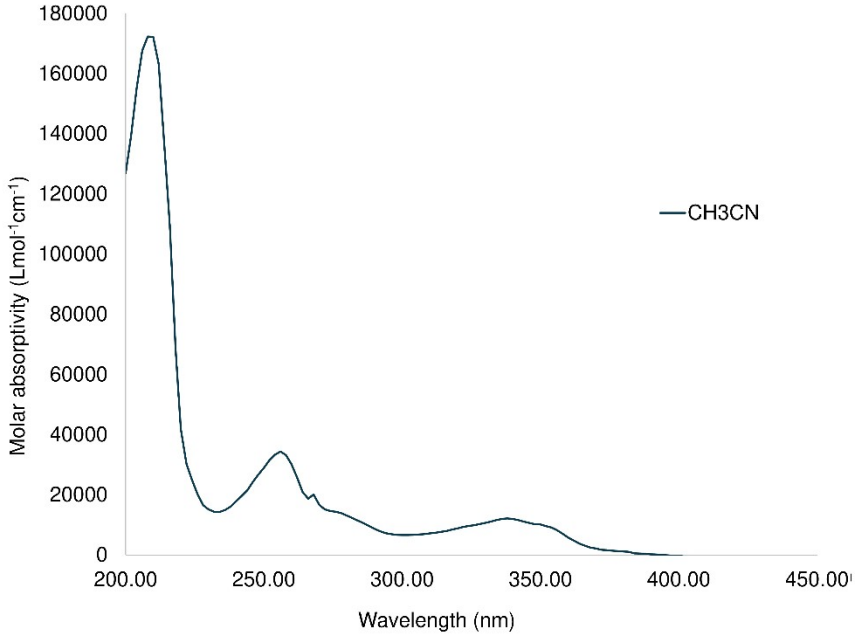

Fig. S12 Electronic absorption spectrum of **1** in acetonitrile.

Table S5 Computed excitation energies (eV), electronic transition configurations and oscillator strengths (*f*) of **1** at B3LYP/6-311+G(2d,p) and CAM-B3LYP/6-311+G(2d,p) level of theories (selected, $f > 0.1$) (Selected)			
Energy (cm^{-1})	Wavelength (nm)	*f*	Major contributions
✓ B3LYP/6-311+G(2d,p)			
30432	328	0.1619	HOMO→LUMO (86%)
31425	318	0.3134	HOMO−1→LUMO (78%)
37403	267	0.4218	HOMO−4→LUMO (27%), HOMO→LUMO+1 (43%)
41289	242	0.1218	HOMO−1→LUMO+1 (58%)
49540	201	0.3976	HOMO−1→LUMO+3 (25%), HOMO−1→LUMO+4 (31%)
✓ CAM-B3LYP/6-311+G(2d,p)			
33296	300	0.4991	HOMO→LUMO (81%)
40628	246	0.7047	HOMO−3→LUMO (21%), HOMO→LUMO+1 (51%)
45104	221	0.1994	HOMO−1→LUMO+1 (51%)
50740	197	0.2625	HOMO→LUMO+4 (35%), HOMO→LUMO+6 (33%)
56454	177	0.1481	HOMO−6→LUMO+1 (22%), HOMO−5→LUMO+2 (31%)

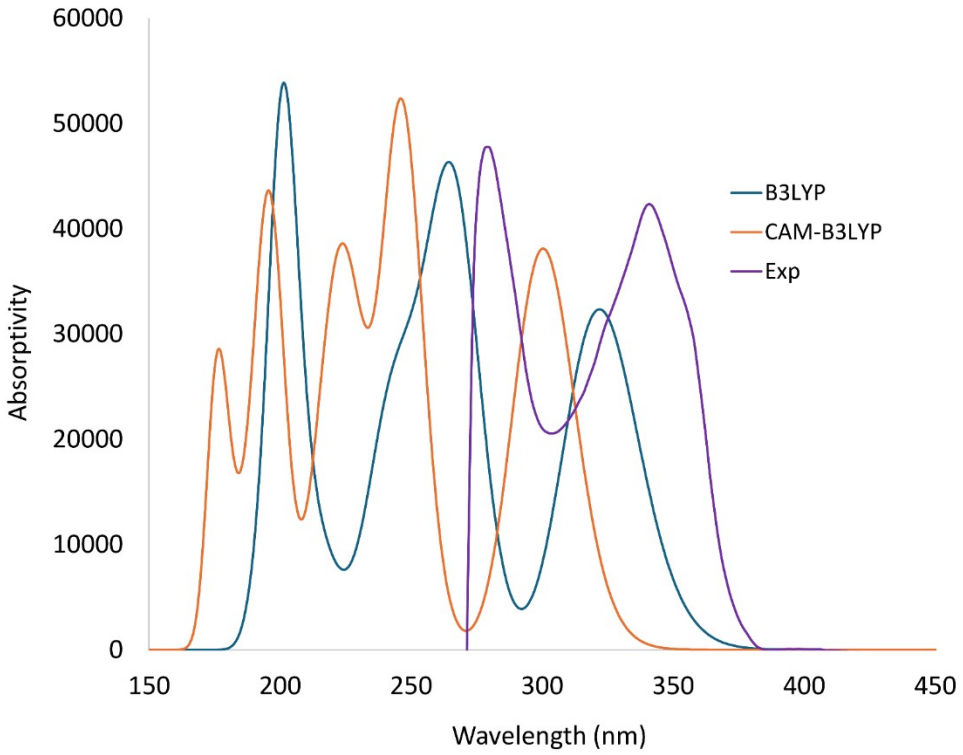

Fig. S13 Theoretical electronic spectra of **1** obtained at both B3LYP/6-311+G(2d,p) and CAM-B3LYP/6-311+G(2d,p) levels of theory in comparison to the experimental one in the same solvent (DMSO).

Table S6 Computed excitation energies (eV), electronic transition configurations and oscillator strengths (*f*) of **2** at B3LYP/LANL2DZ and CAM-B3LYP/LANL2DZ level of theories (selected, $f > 0.1$, except for the lowest energy transitions) (Selected)

Energy (cm^{-1})	Wavelength (nm)	*f*	Major contributions
✓ B3LYP/LANL2DZ			
19519	512	0.0019	HOMO→LUMO (99%)
21305	469	0.0712	HOMO−1→LUMO (98%)
23531	424	0.0052	HOMO−2→LUMO (94%)
25892	386	0.0264	HOMO−3→LUMO (79%)
27747	360	0.3492	HOMO−4→LUMO (75%)
31252	319	0.0684	HOMO−1→LUMO+1 (85%)
32121	311	0.0694	HOMO→LUMO+2 (68%)
36116	276	0.1943	HOMO−8→LUMO (38%), HOMO−3→LUMO+1 (31%)
39205	255	0.2102	HOMO−4→LUMO+1 (25%), HOMO−4−LUMO+2 (26%)
✓ CAM-B3LYP/LANL2DZ			
24724	404	0.0011	HOMO→LUMO (96%)
26183	381	0.1088	HOMO−1→LUMO (96%)
28461	351	0.0084	HOMO−2→LUMO (85%)
30122	331	0.2043	HOMO−3→LUMO (81%)
30834	324	0.3152	HOMO−4→LUMO (89%)
38283	261	0.1227	HOMO−6→LUMO (23%)
39342	254	0.2125	HOMO−3→LUMO+1 (20%)
40483	247	0.2102	HOMO→LUMO+2 (35%)
43125	231	0.1802	HOMO−8→LUMO (23%)

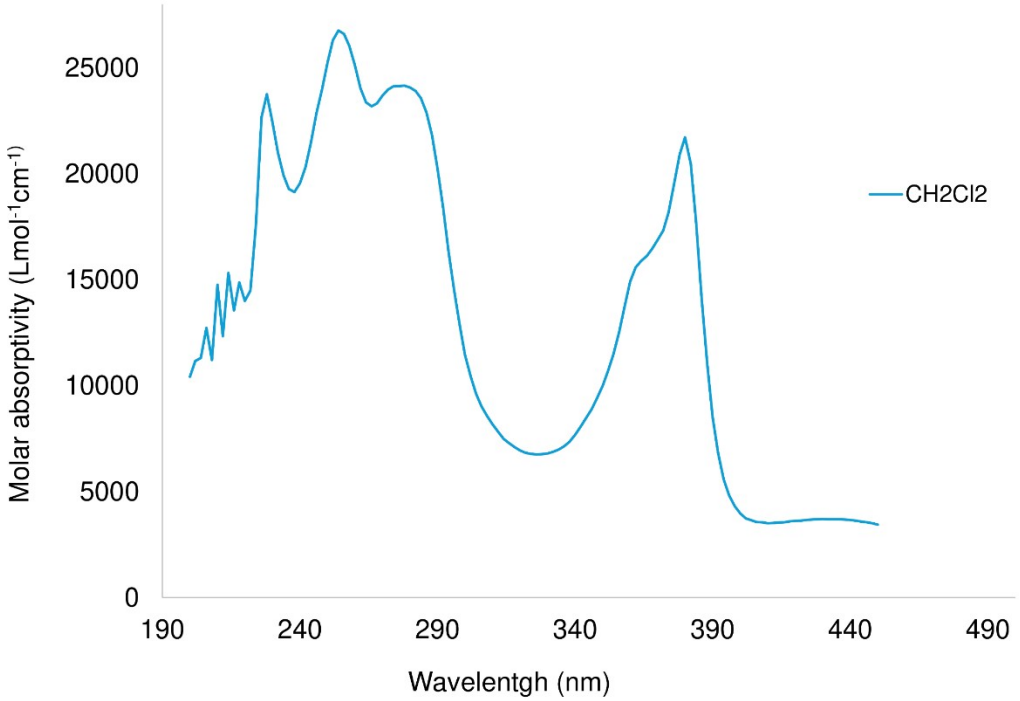

Fig. S14 Electronic absorption spectrum of **1** in dichloromethane.

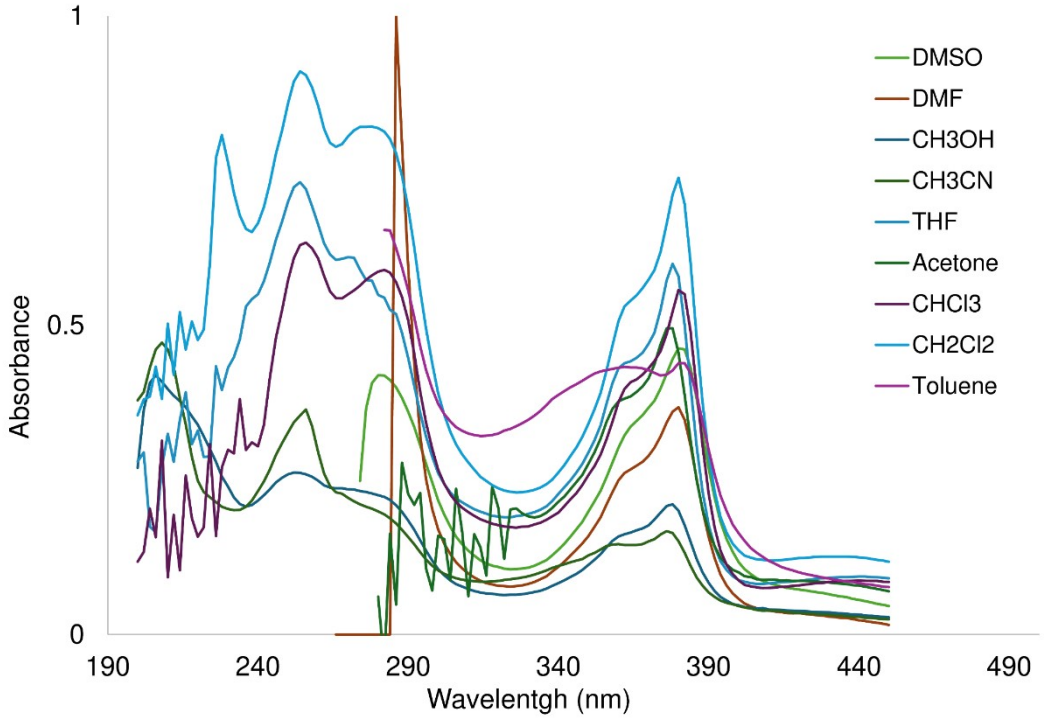

Fig. S15 Electronic absorption spectra of **2** in solvents of different polarities and hydrogen bond tendency (cutoff of the solvents are considered in the drawing of the electronic spectra).

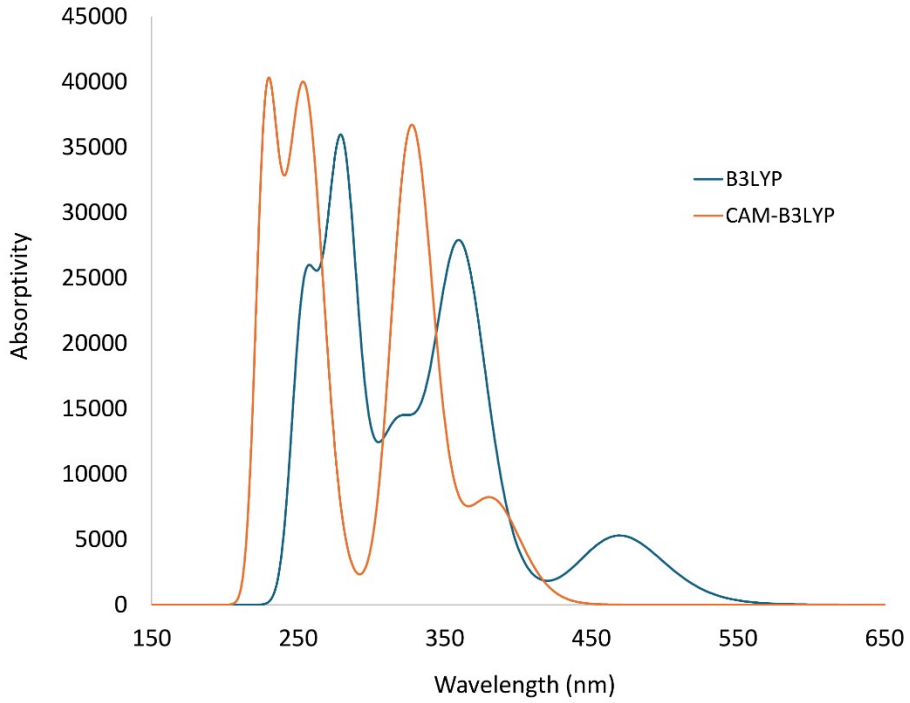

Fig. S16 Theoretical electronic spectra of **2** obtained at both B3LYP/LANL2DZ and CAM-B3LYP/LANL2DZ level of theories.

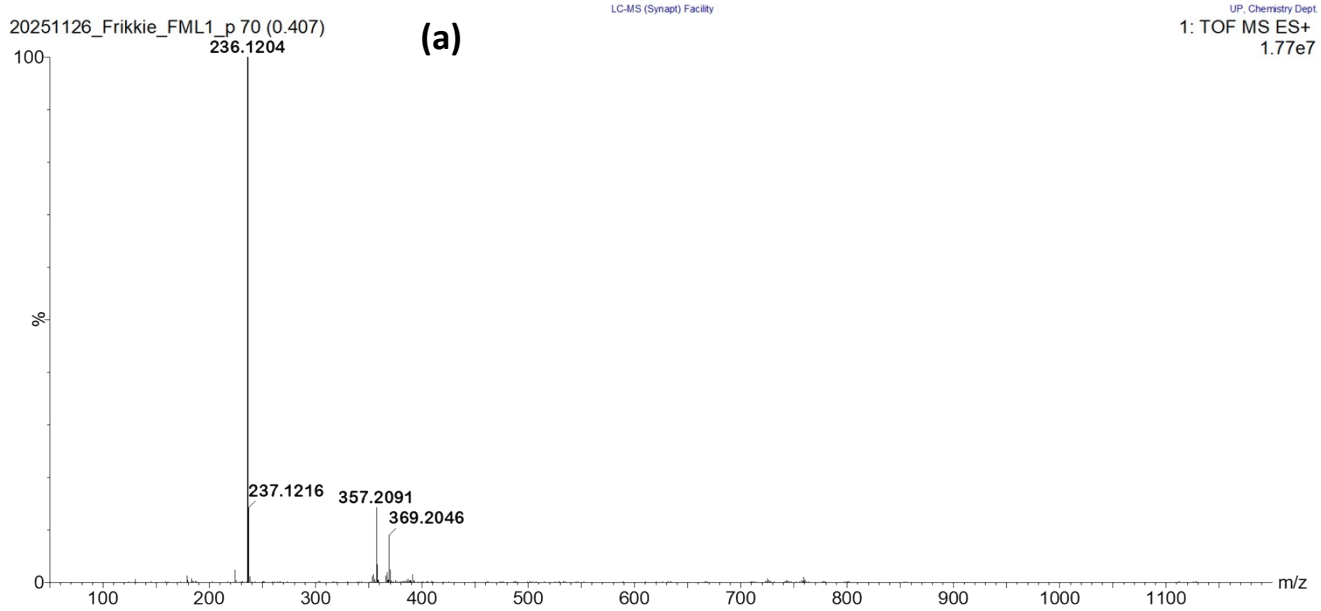
LC-MS (Synapt) Facility
UP, Chemistry Dept.
20251126_Frikkie_FML1_p 70 (0.407)
(a)
1: TOF MS ES+
1.77e7
236.1204
237.1216
357.2091
369.2046
%
m/z

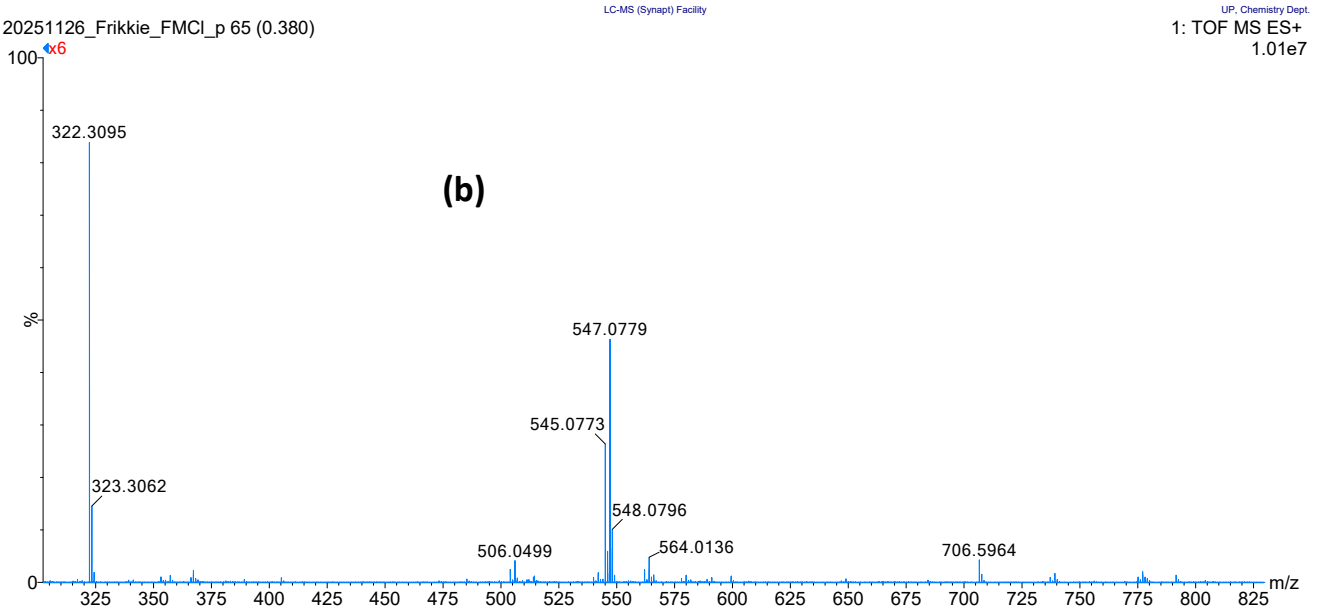
LC-MS (Synapt) Facility
UP, Chemistry Dept.
20251126_Frikkie_FMCl_p 65 (0.380)
1: TOF MS ES+
1.01e7
x6
(b)
322.3095
323.3062
506.0499
545.0773
547.0779
548.0796
564.0136
706.5964
%
m/z

Fig. S17 HR-MS of **1** (a) and **2** (b).